Isoleucine epimerization kinetics in the shell of *Arctica islandica*

JOHN-ERIK HAUGEN & HANS PETTER SEJRUP

Haugen, J.-E. & Sejrup, H. P.: Isoleucine epimerization kinetics in the shell of *Arctica islandica*. *Norsk Geologisk Tidsskrift*, Vol. 72, pp. 171–180. Oslo 1992. ISSN 0029-196X.

Isoleucine epimerization in the two main shell layers of the bivalve *Arctica islandica* has been studied in heated modern samples and fossil samples. The derived Arrhenius parameters are similar to previously reported data on calcareous organisms. Reactions taking place in heated modern shell are essentially in agreement with diagenetic processes taking place during natural aging of *Arctica* shells at ambient temperatures. Hydrolysis rate exceeded epimerization rate of bound isoleucine over the entire temperature range from 0–160 C, suggesting preferential epimerization of terminal isoleucine. The two shell layers showed a significant difference in isoleucine epimerization rate. The lower epimerization rate of the inner layer is ascribed to a lower hydrolysis rate, possibly due to a lower water content in the inner layer. Accordingly, shell layering should be taken into consideration when fossil shells are being used for dating Quaternary sedimentary deposits and sampling strategies should be developed to restrict analyses to a single structural layer.

John-Erik Haugen, Section for Chemical Analysis, National Institute of Public Health, Geitmyrsveien 75, N-0462 Oslo 4, Norway; Hans Petter Sejrup, Department of Geology, Section B, Allégaten 41, 5007, Bergen, Norway.

Amino acid racemization has become an important tool in geochronology and paleothermometry of Quaternary deposits. The dating technique is based on the diagenetic conversion of the protein amino acid L-isoleucine (Ile) to the non-protein amino acid D-alloisoleucine (aIle). Essentially, all of the isoleucine occurs in the L-configuration in the carbonate of living shells. The conversion of L-Ile to D-aIle (epimerization) takes place within carbonate fossils after burial and the amount of alloisoleucine increases relative to isoleucine with increasing age of the fossil. The reaction proceeds until an equilibrium is reached at an aIle/Ile ratio of about 1.3. The isoleucine epimerization process is primarily controlled by temperature and age and follows reversible first-order kinetics.

Fossil specimens of the mollusk species *Arctica islandica* have frequently been used for dating Quaternary marine sediments by means of the isoleucine epimerization reaction (Miller et al. 1983, 1987; Miller & Mangerud 1985; Bowen & Sykes 1988; Sejrup et al. 1987). So far, no kinetic parameters for the isoleucine epimerization reaction have been determined for this species. The aim of this study has been to determine the kinetics for the isoleucine epimerization reaction in order to estimate absolute ages and paleotemperatures of fossil *Arctica* samples. Because of intrashell variation in epimerization throughout the shell layers (Sejrup 1985; Sejrup & Haugen in press), we have, for practical reasons, restricted our kinetic study to each of the two main shell layers of *Arctica islandica*.

Material and methods

Arctica islandica

The mollusk *Arctica islandica* is distributed in coastal waters through the boreal Atlantic and is frequently found within Quaternary marine deposits in NW Europe. It is one of the longest-lived members of the animal kingdom, exceeding the lifespan of the most longevous tortoises (Jones 1983). The shell structure of *Arctica islandica* consists of two distinct aragonitic layers with a homogeneous microstructure (Ehrenbaum 1885; Bøggild 1930; Taylor et al. 1969, 1977) (Fig. 1). The inner layer makes up the major part of the hinge and decreases gradually in thickness towards the pallial line, whereas the outer layer increases in thickness with increasing distance from the hinge, constituting the whole shell structure distal to the pallial line. In this study we have focused on the epimerization kinetics of these two individual layers.

Heating experiments

In order to estimate absolute ages and paleotemperatures of fossil samples, the kinetic equation for the isoleucine epimerization reaction must be known. This can be attained by exposing modern shell samples to elevated temperatures at different time intervals. Results from the heating experiments together with data from dated fossils whose temperature history is well known are used to obtain the kinetic equations for the epimerization reaction.

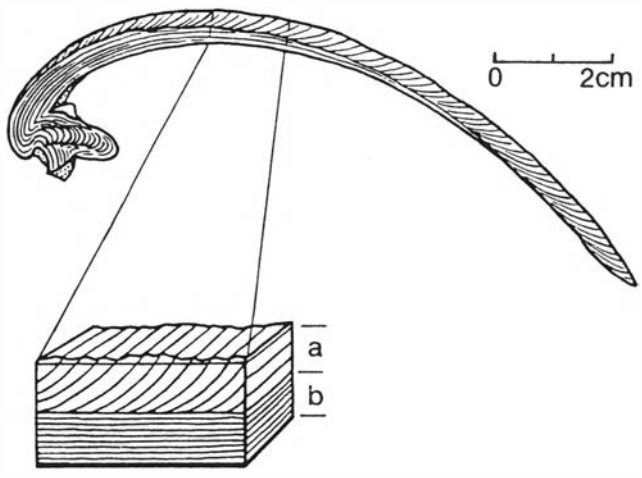

Fig. 1. Idealized cross-section from the umbo to the ventral margin through the central region of an *Arctica* shell. The magnified cross-section indicates the distribution of banding in the outer and inner layers.

Valves of modern specimens of *Arctica*, taken from the western Norwegian coast, were cut into several parts along the umbo to the ventral margin. Each part was exposed to temperatures between 80–160°C for different time periods in sealed 400 ml thick-walled Duran glass tubes. The heating experiments were carried out under water vapor conditions. This was done by placing a tube with 10 ml distilled water into the Duran glass tube prior to sealing. The ratio of free space to sample space was approximately 50:1. Experimental oven temperatures were constant within ±0.5°C. Equilibration time for the tubes to reach the experimental temperature was less than 30 minutes.

Amino acid analysis

At the end of the heating period shells were prepared for amino acid analysis as follows. Shell layers were separated with a dental tool and subsamples of each layer were washed in distilled water under ultrasonication and exposed to 0.1 N hydrochloric acid (1 ml/100 mg shell) for one hour. This was done in order to remove possible surficial contaminants. After acid treatment, samples were washed three times with double distilled water and dried at room temperature. Dried samples were pulverized with a mortar and homogenized. The extent of isoleucine epimerization was determined both on the total hydrolyzed (free + bound) and the free fraction. Hydrolysis was performed with 7 N HCl (0.02 ml/mg shell) at 110°C for 22 hours under nitrogen. The hydrolyzate was evaporated to dryness and redissolved with 0.01 N HCl. Free amino acid samples were dissolved in 7 N HCl, evaporated to dryness and redissolved with 0.01 N HCl. Norleucine was used as internal standard. Amino acid analyses were carried out on a HPLC ion-exchange system with post-column OPA fluorescence detection, using citrate buffers with increasing pH as the mobile phase.

Results and discussion

Isoleucine epimerization

The integrated first-order rate equation for the epimerization reaction is expressed as:

$$1.77k_1 t = \ln \frac{(1 + \text{aIle/Ile})}{(1 - (k_2/k_1)\text{aIle/Ile})} - \ln \frac{(1 + \text{aIle/Ile}_0)}{(1 - (k_2/k_1)\text{aIle/Ile}_0)} \quad (1)$$

t is the heating time (age of sample), and $k_2/k_1 = 1/1.3$ (Williams & Smith 1977; McCoy 1987). The initial aIle/Ile ratio of a modern shell sample will be greater than zero due to a small amount of epimerization induced by the hydrolysis procedure during sample preparation. For modern *Arctica* samples this initial aIle/Ile ratio (aIle/Ile$_0$) of the total fraction is 0.016 for the outer layer and 0.011 for the inner layer (Haugen & Sejrup 1990). Reported initial aIle/Ile ratios of modern mollusks vary between 0.011 and 0.018 (Mitterer 1975; McCoy 1987; Miller & Hare 1980; Miller 1985; Haugen & Sejrup 1990). Our values gave integration constants (second term in equation 1) of 0.019 (inner layer) and 0.028 (outer layer). By inserting the known values and solving for k_1 the forward rate constant reduces to:

$$k_1 = \frac{\ln[(1 + \text{aIle/Ile})/(1 - 0.77\text{aIle/Ile})] - 0.028}{1.77t} \quad (2)$$

The measured aIle/Ile ratios for *Arctica* subjected to elevated temperatures from 80 to 160°C for various

Table 1. Measured aIle/Ile ratios of the outer layer of heated *Arctica* shell. Each number is a mean of at least three parallel samples (S.D. ≤ 7%).

Temp. (°C)	Time (hrs)	aIle/Ile (tot)	aIle/Ile (free)	aIle/Ile (bound)
80	1010	0.045	0.381	0.039
	1500	0.061	0.451	0.053
100	147	0.054	0.336	0.080
	640	0.198	0.587	0.118
120	40	0.064	0.314	0.040
	90	0.110	0.499	0.077
	162	0.205	0.569	0.145
	245	0.269	0.626	0.204
140	5	0.044	0.340	0.034
	10	0.074	0.423	0.057
	26	0.170	0.507	0.110
	38	0.233	0.551	0.155
	56	0.328	0.606	0.199
	75	0.434	0.695	0.264
	98	0.499	0.755	0.354
	125	0.576	0.835	0.436
	145	0.639	0.910	0.485
	195	0.768	1.000	0.600
	240	0.876	1.037	0.671
	285	0.912	1.058	0.733
	336	0.959	1.095	0.780
	407	1.007	1.125	0.846
160	2	0.081	0.196	0.053
	3	0.110	0.446	0.074
	4	0.130	0.571	0.090
	24	0.768	0.955	0.586
	45	0.844	1.146	0.812

Table 2. Measured aIle/Ile ratios of the inner layer of heated *Arctica* shell. Each number is a mean of at least three parallel samples (S.D. ≤ 7%).

Temp. (°C)	Time (hrs)	aIle/Ile (tot)	aIle/Ile (free)	aIle/Ile (bound)
80	1010	0.030	0.224	0.026
	1500	0.037	0.312	0.036
100	147	0.040	0.212	0.025
	640	0.098	0.478	0.069
120	40	0.042	0.258	0.025
	90	0.082	0.353	0.045
	162	0.145	0.428	0.080
	245	0.229	0.523	0.135
140	5	0.030	0.148	0.025
	10	0.057	0.367	0.040
	26	0.124	0.415	0.090
	38	0.164	0.461	0.118
	56	0.235	0.541	0.160
	75	0.305	0.617	0.210
	98	0.400	0.674	0.261
	125	0.473	0.756	0.325
	145	0.534	0.813	0.375
	195	0.643	0.875	0.476
	240	0.743	0.917	0.563
	285	0.787	0.945	0.611
	336	0.834	0.965	0.661
	407	0.887	1.010	0.715
160	2	0.050	0.108	0.035
	3	0.081	0.387	0.064
	4	0.102	0.495	0.090
	24	0.686	'0.861	0.475
	45	0.745	0.968	0.598

lengths of time are given in Tables 1 and 2. A significant difference in the extent of isoleucine epimerization is observed for the two layers in all three fractions (total, bound and free). A higher apparent reaction rate is demonstrated for the outer layer and the absolute difference in aIle/Ile ratios between the layers seems to increase with time. The difference in extent of epimerization varies between 10 to 40% relative to the inner layer. Reaction rates (k_1), calculated from the aIle/Ile ratios (Tables 1 and 2) and equation 2 for the different fractions are given in Table 3. As in most chemical reactions, the reaction rate is strongly temperature dependent. An increase of 20°C causes a 4–5 times increase in the rate constant (Table 3).

Detailed kinetic curves for the epimerization of isoleucine in *Arctica*, based on more closely spaced heating times at 140°C are presented in Figs. 2 and 3. The highest extent of isoleucine epimerization is seen in the free fraction followed by the total and bound fraction. The shape of the epimerization curves is similar to kinetic curves from other studies on isoleucine epimerization in carbonate systems such as mollusks and foraminifera (Lajoie et al. 1980; Kriausakul & Mitterer 1980a, 1980b; Müller 1983; Bada & Schroeder 1972; McCoy 1987). Our epimerization curves are characterized by two to three linear segments of different slopes joined by a transition zone. Linear first-order kinetics of the total fraction are followed to an aIle/Ile ratio of about 0.45 in the outer and 0.4 in the inner layer. Previously reported ranges of the first linear segment in mollusks vary between 0.3 and 0.4 in aIle/Ile ratio (Kriausakul & Mitterer 1980a; Wehmiller 1980, 1982; McCoy 1987). The variability of the first transition point may be due to generic variation in amino acid composition or temperature (King & Neville 1977; Wehmiller 1980; Lajoie et al. 1980). The second inflection points are about 0.9 and 0.8, which agree with the species *Mercenaria* (Kriausakul & Mitterer 1980b).

It has been demonstrated that the slowest epimerization of isoleucine occurs when isoleucine exists in the free state, whereas the highest rate is found in the bound state (Kriausakul & Mitterer 1978, 1980b). Consequently, a significant extent of epimerization of isoleucine must occur in internal bound or at terminal positions during hydrolysis to account for the extensively epimerized

Table 3. Rate constants for isoleucine hydrolysis (k_{hyd}) and isoleucine epimerization in the bound (k_{epb}) and total (k_{ept}) fraction. The hydrolysis rate constants have been calculated from the expression $kt = \ln[1/(1-x)]$, where k is the rate constant and x is the fraction of hydrolysis at time t. Letters *A* and *B* refer to 4800 and 12,000-year-old fossil *Arctica* samples which have experienced a diagenetic temperature of about 8.5°C (Miller et al. 1987).

Temp. (°C)	k_{hyd} (yr^{-1})	k_{ept} (yr^{-1})	k_{epb} (yr^{-1})	k_{epb}/k_{hyd}
Outer layer				
80	0.50 ± 0.01	0.25 ± 0.01	0.21 ± 0.01	0.42
100	1.95 ± 0.02	2.21 ± 0.04	1.34 ± 0.42	0.68
120	8.05 ± 0.71	9.62 ± 0.81	6.15 ± 0.70	0.76
140	37.65 ± 1.20	50.34 ± 1.50	31.35 ± 0.61	0.83
160	186.03 ± 2.21	276.50 ± 5.60	164.56 ± 3.51	0.88
Fossils				
A	8.50×10^{-6}	5.31×10^{-6}	3.32×10^{-6}	0.39
B	6.40×10^{-6}	4.63×10^{-6}	3.14×10^{-6}	0.49
Inner layer				
80	0.22 ± 0.05	0.15 ± 0.10	0.13 ± 0.01	0.59
100	1.00 ± 0.21	1.27 ± 0.09	0.77 ± 0.01	0.77
120	3.93 ± 0.04	7.11 ± 0.45	3.17 ± 0.12	0.81
140	29.90 ± 1.20	35.74 ± 0.90	24.84 ± 1.76	0.83
160	112.10 ± 8.30	189.66 ± 18.5	104.61 ± 4.56	0.93
Fossils				
A	6.56×10^{-6}	3.11×10^{-6}	2.28×10^{-6}	0.35
B	4.45×10^{-6}	2.90×10^{-6}	1.74×10^{-6}	0.39

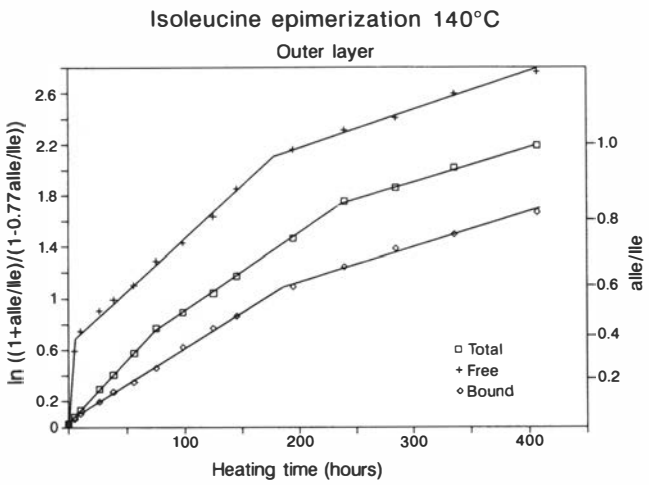

Fig. 2. Isoleucine epimerization at 140 °C in the total, bound and free fraction of the outer layer of *Arctica*.

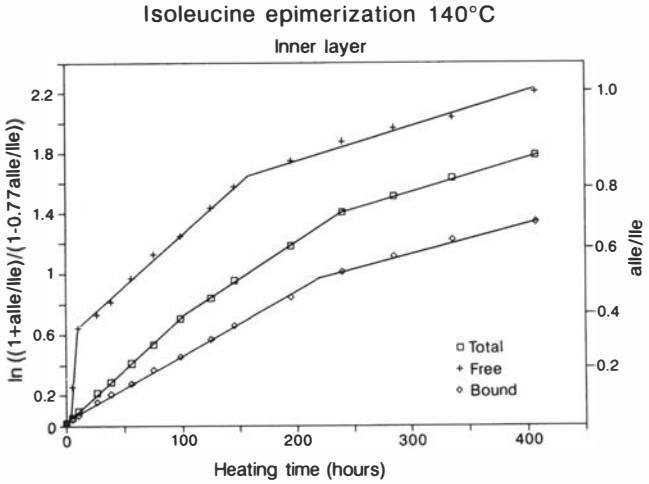

Fig. 3. Isoleucine epimerization at 140 °C in total, bound and free fraction of the inner layer of *Arctica*.

isoleucine observed in the free fraction. This is in accordance with the epimerization hypothesis proposed by several authors (Wehmiller 1971; Wehmiller & Hare 1971; Hare 1971; Hare & Hoering 1973; Kriausakul & Mitterer 1978, 1980b). They explained the more extensive epimerization of free isoleucine as being due to preferentially epimerized isolucine in the terminal position of proteins or peptides. Partial hydrolysis of proteins and peptides to the more slowly epimerizing free amino acids causes a decrease in the first-order rate constant with time. Accordingly, the kinetic curve is controlled by the rate at which isoleucine is transferred from the faster epimerizing terminal position to the slowly epimerizing free state. The first two portions of the kinetic curve will be controlled by the epimerization of terminal and, to some extent, interior isoleucine, whereas the third portion is entirely dominated by the epimerization rate of free isoleucine (Kriausakul & Mitterer 1978).

Arrhenius parameters

The linear relationship between $\ln k_1$ and $1/T$ is expressed by the Arrhenius equation:

$$\ln k_1 = \ln A - E_a/RT \quad (3)$$

where A is the frequency factor
E_a the activation energy
R the gas constant (1.9872 cal/mol)
T is the absolute temperature (K)

To provide control for the epimerization at lower temperatures, aIle/Ile ratios of radiocarbon-dated fossil shells have been used. Radiocarbon-dated shell samples of Holocene and latest Weichselian age from coastal sites in western Scotland, where the effective diagenetic temperature has been estiamted to the present local mean annual temperature as 8.5°C (Miller et al. 1987), were used together with the high-temperature data for the Arrhenius plot (Table 3). It is assumed that the relationship expressed by equation 3 is linear over the entire studied temperature range (0–160°C) and that the reaction mechanism is the same over this region. A least-squares linear regression of the $\log k_1$ data of the total fraction plotted against their reciprocal absolute temperature yielded the equations:

$$\text{Outer layer: } \log k_1(\text{yr}^{-1}) = 16.78 - 6196/T \quad (4)$$

$$\text{Inner layer: } \log k_1(\text{yr}^{-1}) = 16.81 - 6278/T \quad (5)$$

The correlation coefficients were $r = 0.99$ for both datasets. This suggests that there is a good agreement between the high- and low-temperature isoleucine epimerization reaction in the total fraction. Accordingly, we may assume that the derived Arrhenius equations are the best first approximation of isoleucine epimerization taking place in the total fraction of fossil *Arctica*. However, it must be emphasized that these equations only apply for the first linear phase of the reaction, i.e. for aIle/Ile ratios less than 0.4 for the inner and 0.45 for the outer layer.

The estimated activation energy values for the initial isoleucine epimerization in the total fraction were 28.3 and 28.7 kcal/mol for the outer and inner layer (Table 4). These are similar to previously reported Arrhenius parameters for isoleucine epimerization in the total fraction of mollusks derived from similar experimental conditions; These ranged from 16.45 to 17.29 in frequency factor (log A) and activation energies between 28.1 and 29.4 kcal/mol (Hare 1974; Mitterer 1975; Miller & Hare 1980; Miller 1985; McCoy 1987). The aIle/Ile ratio of the total fraction is a measure of epimerization in various states (proteins, peptides and free amino acids). Accordingly, the derived activation energy is an average of the actual E_a for each of the different states of the amino acid, but will be dominated by the E_a of the fastest proceeding epimerization of isoleucine in terminal positions.

Isoleucine hydrolysis

Ratios between isoleucine epimerization rate in the bound fraction (k_{epb}) and hydrolysis rate (k_{hyd}), suggest that the isoleucine hydrolysis rate exceeds the epimeriza-

Table 4. Calculated frequency factors (log A) and activation energies (E_a) for isoleucine epimerization in the total and bound fraction and isoleucine hydrolysis. The numbers shown for epimerization in the total fraction are based on linear regression of high- and low-temperature data whereas the data shown for epimerization and hydrolysis of the bound fraction are based on the high-temperature data only.

Reaction	Outer layer		Inner layer	
	log A	E_a (kcal/mol)	log A	E_a (kcal/mol)
Epim. (tot)	16.8	28.3	16.8	28.7
Epim. (bound)	14.8	25.1	14.8	25.6
Hydrolysis	13.4	22.4	14.1	24.1

tion rate in the bound state over the entire temperature range from 8.5 to 160°C (Table 3). According to these rate ratios, k_{hyd} is about 1.4 times greater than k_{epb} in heated samples, whereas it is about 2.5 times greater in the fossil samples. Consequently, epimerization in the bound fraction of fossil samples proceeds at a slower rate relative to hydrolysis rate than in heated samples. This is probably due to a different temperature dependency of these two reactions, as suggested by Kriausakul & Mitterer (1980a). This is supported by the difference in activation energies of the two processes (Table 4), and increasing k_{epb}/k_{hyd} ratios with increasing temperature (Table 3). Even though the hydrolysis and epimerization in the bound state seem to proceed at somewhat different relative rates at both experimental and natural temperatures, this does not seem to have any significant effect on the overall rate of epimerization in the total fraction which shows a good linear correlation with temperature. This suggests that the enhanced extent of hydrolysis (giving rise to highly epimerized isoleucine) relative to epimerization in the bound state in fossil samples could compensate for the decreased epimerization observed in the bound fraction. Kriausakul & Mitterer (1980a) demonstrated higher epimerization rates in the bound fraction relative to the hydrolysis rate over the entire temperature range from 0 to 152°C. Their results were based on heating experiments of a dipeptide carried out in a water solution. Fossil shells, however, consist of several protein components which are converted into a number of peptides of different molecular weight fractions with time through proceeding partial hydrolysis. It is therefore questionable whether reaction rates measured on simple dipeptides are directly comparable to the values obtained from fossil shells.

Linear regression of the high-temperature k_{hyd} and k_{epb} data shows a poor linear correlation with the fossil data ($r = 0.63$). This suggests that the high-temperature experiment did not adequately simulate these two processes acting on geological time-scales at ambient temperatures. However, the epimerization in the total fraction shows a good linearity between high-temperature and fossil data. Accordingly, dating or temperature estimates based on isoleucine epimerization in the total fraction of fossil samples should be justified. Because of the poor linearity between the fossil and the high-temperature data for hydrolysis and epimerization in the bound fraction (Table 4), we used the high-temperature data only for calculating the Arrhenius parameters for these two processes.

It is assumed that the experimental data will reflect the relative difference in reaction rates between the two shell layers. Both layers have similar frequency factors for hydrolysis and epimerization in the bound and total fraction. However, the activation energies are all somewhat higher in the inner layer, the highest difference being found for the activation energy of hydrolysis. Hare (1976) found activation energies for hydrolysis of amino acids in gelatin of 22–23 kcal/mol, whereas Kriausakul & Mitterer (1978) found 21–23 kcal/mol for a dipeptide. These results are similar to our values from *Arctica* shell protein.

It is noteworthy that the difference in activation energy for hydrolysis of the two layers is about 2 kcal/mol; This is substantially greater than the differences observed in activation energies for isoleucine epimerization in the total and bound state. McCoy (1987) determined the error in determining the activation energy to be 0.7 kcal/mol. This suggests that the difference in activation energy for isoleucine hydrolysis between the two layers is statistically significant. Consequently, we conclude that the lower extent of isoleucine epimerization in the inner layer may essentially be ascribed to the higher activation energy of hydrolysis of isoleucine in the bound state. This is consistent with the observed higher extent of epimerization in the outer layer, since enhanced hydrolysis would cause an increased transfer of isoleucine to rapidly epimerizing terminal positions (Kriausakul & Mitterer 1978, 1980b). A higher hydrolysis rate in the outer layer has been demonstrated in fossil *Arctica* data by Sejrup & Haugen (in press). This indicates that the polypeptides of the inner layer are more stable towards hydrolysis.

Diagenetic changes in amino acid composition

Amino acid concentrations

During the early stage of amino acid diagenesis in calcareous organisms, a rapid decline in total amino acid content is normally observed, followed by a plateau of gradually decreasing amino acid content at later stages (Wehmiller 1980; Miller & Hare 1980). Figure 4 shows the decrease in total amino acid content in the outer layer with increasing extent of diagenesis expressed by increasing aIle/Ile ratios for both pyrolyzed and fossil samples. A similar distribution was found for the inner layer. This suggests that there is a rapid loss of more labile amino acid components during the early stage of diagenesis. The later stage may reflect degradation of more resistant amino acid material, comprising about 40% of the initial total concentration. The loss could be due to a combination of several degradation pathways such as decarboxylation and deamination or leaching (Vallentyne 1964; Hare 1974; Bada et al. 1978).

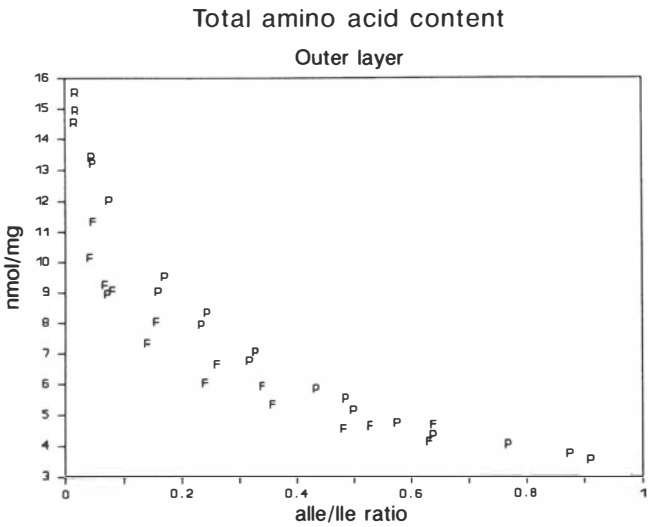

Fig. 4. Distribution of total concentration of amino acids in recent (R), fossil (F) and pyrolyzed (P) shell samples with increasing extent of isoleucine epimerization.

In both layers a more pronounced decrease is observed in fossil samples relative to pyrolyzed samples during the early stage of diagenesis. This suggests that the heating experiments do not quite duplicate the early natural decomposition processes. Several factors could explain this discrepancy between heated and fossil samples; It has been demonstrated that water may have the most significant effect on different decomposition reactions of proteins and amino acids (Vallentyne 1964, 1969; Hare 1974; Bada et al. 1978). Our heating experiments were carried out in water vapor, whereas fossil samples are normally completely saturated with water during the early diagenesis. We therefore believe, that the fossil shells could have been exposed to a higher amount of water than the pyrolyzed samples, probably enhancing the decomposition of amino acids during the early diagenesis (including leaching).

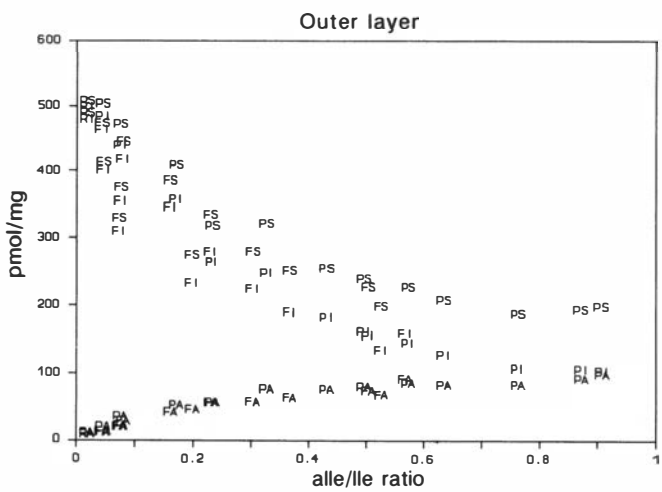

Fig. 5. Distribution of alloisoleucine, isoleucine and alloisoleucine + isoleucine in heated and fossil samples with increasing extent of isoleucine epimerization. Letters are as follows: R – recent; F – fossil; P – pyrolyzed; A – alloisoleucine; I – Isoleucine; S – sum of aIle and Ile.

The concentrations of total alloisoleucine, isoleucine and alloisoleucine + isoleucine in the outer layer are presented in Fig. 5, from both pyrolyzed and fossil samples. A similar distribution was found in the inner layer. No significant difference is observed in the distribution of alloisoleucine and isoleucine for pyrolyzed and fossil samples, suggesting that the heating experiment to a great extent parallels the natural aging of isoleucine.

Total aIle + Ile concentrations are highest in recent samples and decrease rapidly by about 40% up to an aIle/Ile ratio of about 0.5 (Fig. 5). The loss of isoleucine is not compensated for by a corresponding increase in alloisoleucine. An increase of alloisoleucine would be expected, assuming a closed system and isoleucine epimerization being the only likely diagenetic pathway of isoleucine. This therefore suggests that a significant loss of both isoleucine and alloisoleucine must take place during diagenesis. It is difficult to assess which processes are responsible for the loss of these compounds since degradation pathways such as decarboxylation and deamination could be involved as well as leaching, or a combintion of both.

Amino acid distribution

We have previously demonstrated that there is no significant difference in amino acid composition between the two shell layers of recent samples of *Arctica islandica* (Haugen & Sejrup 1990). We observed a significant change in amino acid compsoition in both layers with increasing diagenesis. Amino acid abundance data from the inner layer showed basically the same pattern as the data from the outer layer. The relative percentages of the more common amino acids in the outer layer have been listed according to increased extent of diagenesis for both heated and fossil samples (Table 5). To investigate systematic changes in amino acid composition with increasing diagenesis we have used SIMCA (Soft Independent Modeling of Class Analogy) principal component analysis (PCA). SIMCA uses the NIPALS algorithm to extract the principal components of a multivariate data set (Kowalski & Bender 1972; Wold 1976). Cross-validation (Wold 1978) was used to determine whether a PC was statistically significant or not. Since the variables in the raw data matrix (Table 5) differed considerably in absolute size, the variables were scaled to equal variance. This was done in order to prevent masking of systematic variation in small variables by the much larger variance in major variables. The data were scaled to equal variance by dividing each variable by its standard deviation (Kowalski & Bender, 1972, 1973; Kvalheim 1985).

Figure 6 shows the projection of the objects (score plot) of the outer layer into the plane described by the first two principal components. A similar distribution was found for the inner layer. The first two PCs were statistically significant, denoting a systematic variance in the data and explained 84.4% of the total variance. It is

Table 5. Amino acid composition of recent (R), pyrolyzed (P) and fossil (F) shell samples from the outer layer listed according to increasing aIle/Ile ratios. Samples labelled *A* to *C* represent parallel samples. Abbreviations are as follows: Asp – aspartic acid; Thr – threonine; Ser – serine; Glu – glutamic acid; Gly – glycine; Ala – alanine; Val – valine; aIle – alloisoleucine; Ile – isoleucine; Leu – leucine.

Obj. Name	aIle/Ile	Asp	Thr + Ser	Glu	Gly	Ala	Val	aIle	Ile	Leu
R0	0.016	23.9	15.0	14.0	14.1	13.8	7.0	0.06	3.6	4.1
P1	0.044	23.1	12.1	14.6	17.0	16.0	7.2	0.12	3.4	3.9
P2	0.074	22.8	8.5	16.9	17.6	18.3	8.2	0.24	3.3	3.4
P3	0.170	20.8	7.1	16.4	17.5	20.6	8.8	0.47	3.2	4.3
P4	0.233	19.3	6.7	17.8	17.0	21.3	9.4	0.68	3.2	4.4
P5A	0.328	19.7	5.7	18.9	19.5	22.3	9.3	1.05	3.0	4.0
P5B	0.320	19.6	4.3	18.7	19.0	20.5	9.8	1.12	2.9	3.8
P5C	0.329	19.6	4.6	18.0	20.0	21.4	10.0	0.96	3.2	4.4
P6	0.434	17.9	3.5	18.5	20.2	22.4	9.3	1.21	2.7	4.3
P7	0.499	17.3	2.7	19.2	20.9	22.3	10.1	1.34	2.7	3.9
P8	0.576	17.9	2.3	19.7	21.3	22.2	10.2	1.57	2.6	4.7
P9	0.639	17.7	2.1	21.3	20.4	22.5	10.2	1.68	2.4	4.9
P10	0.768	16.8	2.2	19.0	19.8	23.1	11.0	1.99	2.3	4.9
F1	0.160	23.0	14.0	15.0	14.8	14.0	9.0	0.11	4.0	3.5
F2	0.200	24.0	12.0	16.1	14.0	14.0	10.0	0.14	3.5	3.4
F3	0.270	21.0	9.1	15.7	14.7	16.0	10.4	0.56	4.3	5.3
F4	0.358	20.0	8.0	15.6	13.8	18.4	9.7	0.83	3.5	4.3
F5	0.369	20.5	8.9	17.0	13.5	16.0	11.1	0.90	3.8	5.0
F6A	0.358	20.0	7.7	17.6	12.3	15.9	12.3	1.13	3.4	4.7
F6B	0.369	19.5	7.5	17.8	11.7	16.8	12.0	1.04	3.2	3.8
F7	0.426	19.5	5.9	18.6	12.6	20.8	12.1	1.14	4.0	4.8
F8	0.441	18.2	6.6	18.1	10.7	18.7	12.1	1.30	3.8	4.8
F9	0.529	18.4	6.0	18.8	11.5	18.6	12.6	1.50	3.4	4.7
F10A	0.561	20.8	3.8	18.5	12.5	22.3	12.9	1.59	3.1	4.8
F10B	0.611	20.2	4.3	18.2	13.0	21.9	12.9	1.74	3.0	4.7

seen that there is a systematic variation in amino acid composition along the first principal component (PC1, 62% variance) associated with increasing aIle/Ile ratios. The most extensive diagenetically altered samples are grouped to the far left. Both heated and fossil samples show the same variation along PC1; however, they are grouped slightly apart along the second principal component (PC2, 24% variance). Comparing objects with similar aIle/Ile ratios, they seem to be equally correlated with both PCs. Correlation of variables with the PCs is visualized by the variable loading plot (Fig. 7). The systematic variation in amino acid composition observed along PC1 is ascribed to changes in aspartic acid (Asp) and threonine + serine (T + S), which show high positive loadings, and glutamic acid (Glu), alanine (Ala) and alloisoleucine (aIle), which show high negative loadings along PC1. Correspondingly, glycine (Gly) and valine (Val) are responsible for the variation along PC2.

The changes observed in the amino acid pattern with increased diagenesis are in agreement with previously reported data from studies on thermal stability of amino acids in calcareous shells and forams (Vallentyne 1969; Hare & Mitterer 1969; Bada et al. 1978; Akiyama 1980; Bada & Man 1980; Miller & Hare 1980; Haugen et al.

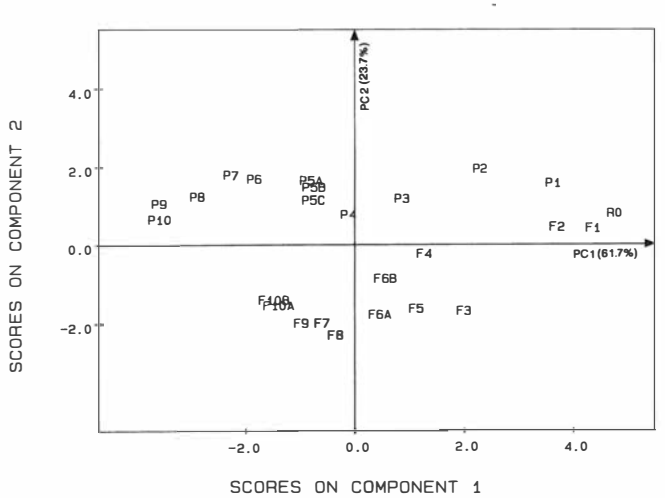

Fig. 6. Object score plot from principal component analysis of amino acid composition data (Table 5). Object names are as in Table 5.

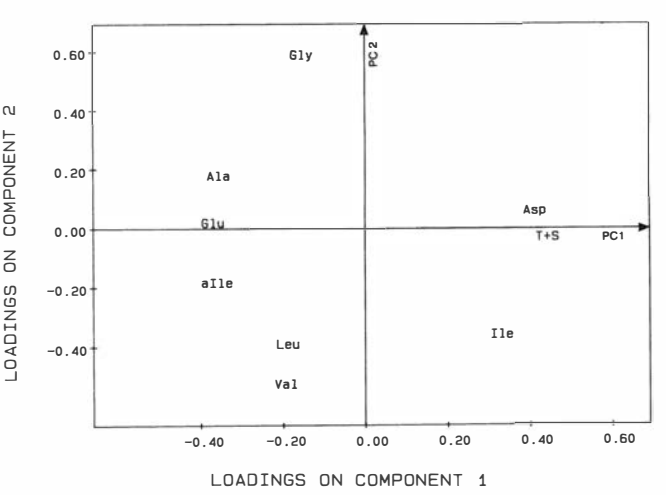

Fig. 7. Variable loading plot from principal component analysis of amino acid composition data (Table 5). Abbreviations as in Table 5. Abbreviation T + S corresponds to Thr + Ser (Table 5).

1989). The enrichment of glutamic acid is probably due to the fact that it is the thermally most stable amino acid compound (Vallentyne 1964). Threonine and serine are known to be the most labile amino acids and show a rapid decrease during early diagenesis (Schroeder & Bada 1977; Bada et al. 1978). The decrease in threonine and serine seems to be slightly delayed in the fossil samples compared to the heated samples of similar aIle/Ile ratio (Table 5). It has been demonstrated that the degradation of these two hydroxy amino acids leads to the production of glycine and alanine (Vallentyne 1969; Bada et al. 1978; Bada & Man 1980). Both heated and fossil samples show decreasing Gly/Ala ratios with increasing diagenesis due to an increase in alanine relative to glycine. This suggests that dehydration of the hydroxy amino acids may be the dominant degradation pathway (Bada et al. 1978). However, the glycine abundance stays fairly stable in the fossil samples, whereas it increases in heated samples. This may indicate that aldol cleavage may also play a role at elevated temperatures (Bada et al. 1978). On the other hand, some glycine could also be accounted for by thermal decomposition of sulfur containing amino acids (Vallentyne 1964). The abundance of aspartic acid decreases slightly in the fossil samples, whereas heated samples show a substantial decrease. This is in agreement with previous heating experiments demonstrating it to be among the most temperature labile amino acid compounds (Vallentyne 1964, 1969; Bada & Man 1980). The primary thermal decomposition pathway of aspartic acid is via deamination to maleic acid and ammonia (Vallentyne 1964, 1969; Bada & Miller 1970). It has been suggested that β-decarboxylation of aspartic acid yielding alanine may be significant (Bada & Man 1980). This reaction would, however, only take place in protein or peptide-bound material. Since aspartic acid is relatively hydrolysis labile, this implies that β-decarboxylation may be of significance only during the earliest stage of diagenesis when most of the aspartic acid is still in the bound state. Accordingly, β-decarboxylation of aspartic acid could partly account for the observed increase in alanine during the early stage of diagenesis.

Cause of intrashell variations in isoleucine epimerization

Several factors may be considered in order to derive an explanation of the observed difference in extent of isoleucine epimerization in the two layers. We have demonstrated that the higher extent of isoleucine epimerization is associated with a higher hydrolysis rate in the outer, relative to the inner layer. It still remains to be explained what causes the enhanced hydrolysis rate in the outer layer. It has been demonstrated that amino acid composition may affect racemization rates (Miller & Hare 1980). This is probably due to the species-specific primary structure of calcified proteins (King & Neville 1977; Smith & Evans 1980). However, amino acid composition of the two layers of *Arctica* are identical (Haugen & Sejrup 1990), and may therefore be ruled out as an explanation for the observed difference in epimerization rate of the two layers. It has also been demonstrated that the presence of calcium-carbonate increases the epimerization rate by enhancing the hydrolysis rate (Kriausakul & Mitterer 1980b). Since the outer layer of the *Arctica* shell has a lower content of protein relative to carbonate (Haugen & Sejrup 1990), this could possibly enhance the hydrolysis rate in the outer layer and thereby increase epimerization of preferentially terminal isoleucine.

Another explanation could be related to a different water content within the shell layers. It is well known that water may have a significant influence on epimerization (Hare 1974; Smith & Evans 1980). We have carried out diffusive reflectance infrared spectra measurements (Kubelka & Munk 1931; Christy et al. 1987) on samples from the two shell structures of *Arctica* (Fig. 8), in order to investigate the distribution of water content within the shell. Three parallel samples of each layer of recent *Arctica* shells were analyzed.

It has previously been demonstrated that the bulk organic matrix of carbonate shells consists of proteins and that only a minor proportion is made up of polysaccharides and lipids (Wada 1964; Degens 1976; Krampitz & Witt 1979; Samata & Krampitz 1982). The band at about 1080 cm^{-1} is typical for undecalcified aragonitic shell which distinguishes it from calcitic shells, and is associated with totally symmetric stretching of C–O bonds (Hotta 1969). The most significant difference between the two layers is observed in the region 1000–1250 cm^{-1}, which probably reflects a higher content of ester groups in the outer layer. The amide-A N-H stretch band normally found in undecalcified shell layers at 3260 cm^{-1} is strong and sharp in shape (Hotta 1969). This absorption band is not seen in our IR spectra. The low O–H stretch absorbance at 1070–1050 cm^{-1} suggests that phenolic groups are insignificant. Accordingly, the O–H stretch band which occurs as a broad band in the 3700–3000 cm^{-1} region may suggest that the amount of water relative to amide-A N–H is significant. The estimated relative difference in absorbance between the

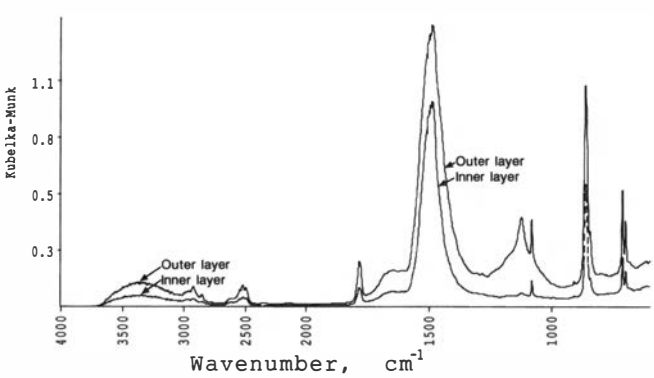

Fig. 8. Infrared spectrum of Kubelka Munk absorbance of the outer and inner layer.

combined protein amide I-II and carboxyl band at 1700–1400 cm^{-1} and the O–H stretch band at 3700–3000 cm^{-1} (Hotta 1969; Williams & Fleming 1980) is about 1.42 for the inner and 2.0 for the outer layer (based on background correction in these regions). Accordingly, this suggests that the water content of the outer layer is about 1.4 times higher than that in the inner layer. Consequently, it is inferred that the higher hydrolysis rate demonstrated in the outer layer may be ascribed to a higher water content relative to protein.

Hudson (1967) suggested that aragonitic layers within shells may contain different amounts of water associated with individual aragonite crystals which may have been trapped during the shell mineralization process. It is difficult to assess to what extent these water molecules could induce partial hydrolysis of the shell proteins. During its living stage and after burial, the shell is exposed to a water saturated environment. We should therefore expect that water would be able to diffuse into the shell structure, in particular, along the layers paralleling the growth lines of the outer layer (Fig. 1) and due to its coarser grained structure compared to the inner layer (Taylor et al. 1969, 1977; Böggild 1930). Diffusion of water into the inner layer would be restricted because of its denser structure and thin banding oriented along the shell (Fig. 1). This may possibly explain the observed differences in water content in the two layers and thus the different epimerization rates.

Conclusions

Heating experiments on modern shells of *Arctica islandica* are useful in understanding the diagenetic processes taking place in the shell on geological time-scales at ambient temperatures. This study has shown that it is essential to compare results from heating experiments with those of fossil proteins to confirm that the heating experiments *de facto* reproduce the reactions in fossils at natural temperatures. We have demonstrated that there are some differences between amino acid diagenesis simulated at high temperatures and diagenesis that occurs under natural conditions. In particular, a difference is demonstrated in the relative rate of hydrolysis and epimerization of bound isoleucine. Nevertheless, there was good agreement between isoleucine epimerization in the total fraction of heated and fossil samples.

The higher extent of isoleucine epimerization in the total fraction of the outer layer relative to the inner layer is essentially the same as that observed in fossil samples. This phenomenon is ascribed to a higher rate of hydrolysis in the outer layer. The enhanced hydrolysis rate may possibly be related to the water content of the shell layer; infrared spectra on undecalcified aragonite from both layers of recent *Arctica* shells suggest a higher water content in the outer layer. Further investigations are needed in order to explain the intrashell gradients in isoleucine epimerization in *Arctica* and to clarify whether a lower water content in the shell layer is a rate-limiting factor in the epimerization process. Our results emphasize that shell-layering should be taken into consideration when fossil shells are being used for dating sedimentary deposits.

Acknowledgments. – This research was supported by the Norwegian Council for Science and the Humanities (NAVF). The authors express their thanks to Professor Gif Miller for critical reading of the manuscript, Dr Alfred Christy at the Chemistry Department for assistance with the IR measurements and Vigdis Clausen Hope for laboratory assistance.

Manuscript received November 1990

References

Akiyama, M. 1980: Diagenetic decomposition of peptide-linked serine residues in the fossil scallop shell. In Hare, P. E., Hoering, T. C. & King, K. Jr. (eds.): *Biogeochemistry of Amino Acids*, 115–128, J. Wiley, New York.

Bada, J. L. & Man, E. H. 1980: Amino acid diagenesis in Deep Sea Drilling Project cores: Kinetics and mechanisms of some reactions and their applications in geochronology and paleotemperature and heat flow determinations. *Earth-Science Reviews 16*, 21–55.

Bada, J. L. & Miller, S. L. 1970: The kinetics and mechanism of the reversible nonenzymatic deamination of aspartic acid. *Journal of the American Chemical Society 92*, 2774–2782.

Bada, J. L. & Scroeder, R. A. 1972: Racemization of isoleucine in calcareous marine sediments: Kinetics and mechanisms. *Earth and Planetary Science Letters 15*, 1–11.

Bada, J. L., Shou, M-Y., Man E. H. & Schroeder, R. A. 1978: Decomposition of hydroxy amino acids in foraminiferal tests; kinetics, mechanism and geochronological implications. *Earth and Planetary Science Letters 41*, 67–76.

Bowen, D. Q. & Sykes, G. A. 1988: Correlation of marine events and glaciations on the northeast Atlantic margin. *Philosophical Transactions of the Royal Society of London, BB 318*, 619–635.

Bøggild, O. B. 1930: The shell structure of mollusks. *Det Kongelige Danske Videnskapelige Selskaps Skrifter 2*, 232–325.

Christy, A. A., Velapoldi, R. A., Karstang, T. V., Kvalheim, O. M., Sletten, E. & Telnæs, N. 1987: Multivariate calibration of diffusive reflectance spectra of coals as an alternative to rank determination by vitrinite reflectance. *Chemometrics and Intelligent Laboratory Systems 2*, 199–207.

Degens, E. T. 1976: Molecular mechanisms on carbonate, phosphate, and silica deposition in the living cell. *Topics of Current Chemistry 64*, 1–112.

Ehrenbaum, E. 1885: Untersuchungen über die Struktur und Bildung der Schale der in der Kieler Bucht häufig vorkommenden Muscheln. *Zeitschrift der wissenschaftlige Zoologie 41*, 1–47.

Hare, P. E. 1971: Effects of hydrolysis on the racemization rate of amino acids. *Carnegie Institution of Washington Yearbook 70*, 256–258.

Hare, P. E. 1974: Amino acid dating – a history and an evaluation. *MASCA Newsletter 10*, 4–7.

Hare, P. E. 1976: Relative reaction rates and activation energies for some amino acid reactions. *Carnegie Institution of Washington Yearbook 75*, 801–806.

Hare, P. E. & Hoering, T. E. 1973: Separation of amino acid optical isomers by gas chromatography. *Carnegie Institution of Washington Yearbook 72*, 690–694.

Hare, P. E. & Mitterer, R. M. 1969: Laboratory simulation of amino acid diagenesis in fossils. *Carnegie Institution of Washington Yearbook 67*, 205–208.

Haugen, J. E. & Sejrup, H. P. 1990: Amino acid composition of aragonitic conchiolin in the shell of *Arctica islandica*. *Lethaia 23*, 133–141.

Haugen, J. E., Sejrup, H. P. & Vogt, N. B. 1989: Chemotaxonomy of Quaternary benthic foraminifera using amino acids. *Journal of Foraminiferal Research 19 (1)*, 38–51.

Hotta, S. 1969: Infrared spectra and conformation of protein constituting the nacreous layer of molluscan shell. *Earth Science; Journal of the Association for Geological Collaboration in Japan 23 (4)*, 133–140.

Hudson, J. D. 1967: The elemental composition of the organic fraction, and the water content of some recent and fossil mollusc shells. *Geochimica et Cosmochimica Acta 31*, 2361–2378.

Jones, D. S. 1983: Sclerochronology: Reading the record of the molluscan shell. *American Scientist 71*, 34–391.

King, K. K. & Neville, C. 1977: Isoleucine epimerization for dating marine sediments: Importance of analyzing monospecific foraminiferal samples. *Science 195*, 1333–1335.

Kowalski, B. R. & Bender, C. F. 1972: Pattern recognition I. A. powerful

approach to interpreting chemical data. *Journal of American Chemical Society 94*, 5632–5639.

Kowalski, B. R. & Bender, C. F. 1973: Pattern recognition II. Linear and non-linear methods for displaying chemical data. *Journal of American Chemical Society 95*, 686–693.

Krampitz, G. & Witt, W. 1979: Biochemical aspects of biomineralization. *Topics of Current Chemistry 78*, 57–144.

Kriausakul, N. & Mitterer, R. M. 1978: Isoleucine epimerization in peptides and proteins: Kinetic factors and application to fossil proteins. *Science 201*, 1011–1014.

Kriausakul, N. & Mitterer, R. M.A 1980a: Comparison of isoleucine epimerization in a model dipeptide and fossil protein. *Geochimica et Cosmochimica Acta 44*, 753–758.

Kriausakul, N. & Mitterer, R. M. 1980b: Some factors affecting the epimerization of isoleucine in peptides and proteins. In Hare, P. E., Hoering, T. C. & King, K., Jr. (eds.): *Biogeochemistry of Amino Acids*, 283–296. J. Wiley, New York.

Kubelka, P. & Munk, F. 1931: Ein Beitrag zur Optik der Farbanstriche. *Zeitschrift für Technische Physik 11a*, 593–743.

Kvalheim, O. M. 1985: Scaling of analytical data. *Analytica Chimica Acta 177*, 71–79.

Lajoie, K. R., Wehmiller, J. F. & Kennedy, G. L. 1980: Inter- and intrageneric racemization kinetics of amino acids in Quaternary mollusks. In Hare, P. E., Hoering, T. C. & King, K. Jr. (eds.): *Biogeochemistry of Amino Acids*, 305–355. J. Wiley, New York.

McCoy, W. D. 1987: The precision of amino acid geochronology and paleothermometry. *Quaternary Science Reviews 6*, 43–54.

Miller, G. H. 1985: Aminostratigraphy of Baffin Island shell-bearing deposits. In Andrews, J. T. (ed.): *Quaternary Environments*, 394–427. Allen & Unwin, Boston.

Miller, G. H. & Hare, P. E. 1980: Amino acid geochronology: Integrity of the carbonate matrix and potential of molluscan fossils. In Hare, P. E., Hoering, T. C. & King, K., Jr. (eds.): *Biogeochemistry of Amino Acids*, 415–443. J. Wiley, New York.

Miller, G. H., Jull, A. J. T., Linick, T., Sutherland, D., Sejrup, H. P., Brigham, J. K., Bowen, D. Q. & Mangerud, J. 1987: Racemization-derived late Devensian temperature reduction in Scotland. *Nature 326*, 593–595.

Miller, G. H. & Mangerud, J. 1985: Aminostratigraphy of European marine interglacial deposits. *Quaternary Science Reviews 4*, 215–278.

Miller, G. H., Sejrup, H. P., Mangerud, J. & Andersen, B. G. 1983: Amino acid ratios in Quaternary molluscs and foraminifera from western Norway: Correlation, geochronology and paleotemperature estimates. *Boreas 12*, 107–124.

Mitterer, R. M. 1975: Ages and diagenetic temperatures of pleistocene deposits of Florida based on isoleucine epimerization in Mercenaria. *Earth and Planetary Science Letters 28*, 275–282.

Müller, 1983: Isoleucine epimerization in Quaternary planktonic foraminifera: Effects of diagenetic hydrolysis and leaching, and Atlantic–Pacific intercore correlations. *Meteor Forschungs-Ergebnisse Reihe C No. 38*, 25–47.

Samata, T. & Krampitz, G. 1982: Ca-binding polypeptides in oyster shells. *Malacologia 22*, 225–233.

Schroeder, R. A. & Bada, J. R. 1977: Kinetics and mechanism of the epimerization and decomposition of threonine in fossil foraminifera. *Geochimica et Cosmochimica Acta 41*, 1087–1095.

Sejrup, H. P. 1985: Amino acid ratios: Not only time and temperature. In Vilks, G. & Syvitski, J. (eds.): *14th Workshop of Arctic Land-Sea Interaction*, 219–223 Bedford, Canada.

Sejrup, H. P., Aaarseth, I., Ellingsen, K. L., Reither, E. & Jansen, E. 1987: Quaternary stratigraphy of the Fladen area, central North Sea: a multidisciplinary study. *Journal of Quaternary Science 2*, 35–58.

Sejrup, H. P. & Haugen, J. E. in press: Amino acid diagenesis in the marine bivalve *Arctica islandica* Linné from NW-European sites: only time and temperature? *Quaternary Science Reviews*.

Smith, G. G. & Evans, R. C. 1980: The effect of structure and conditions on the rate of racemization of free and bound amino acids. In Hare, P. E., Hoering, T. C. & King, K. Jr. (eds.): *Biogeochemistry of Amino Acids*, 257–282. J. Wiley, New York.

Taylor, J. D., Kennedy, W. J. & Hall, A. 1969: The shell structure and mineralogy of the bivalvia. Introduction. Nuculacea-Trigonacea. *Bulletin of the British Museum, Zoology Suppl. 3*, 1–125.

Taylor, J. D., Kennedy, W. J. & Hall, A. 1977: The shell structure and mineralogy of the bivalvia II. Lucinacea-Clavagellacea conclusions. *Bulletin of the British Museum, Zoology 22 (1971–1973)*, 256–294.

Vallentyne, J. R. 1964: Biogeochemistry of organic matter – II. Thermal reaction kinetics and transformation products of amino compounds. *Geochimica et Cosmochimica Acta 28*, 157–188.

Vallentyne, J. R. 1969: Pyrolysis of amino acids in Pleistocene Mercenaria shells. *Geochimica et Cosmochimica Acta 33*, 1453–1458.

Wada, K. 1964: Studies on the mineralization of calcified tissue in molluscs. VII. Histological and histochemical studies of organic matrices in shells. *Bulletin of the National Pearl Research Laboratory 9*, 1078–1086.

Wehmiller, J. F. 1971: Amino acid diagenesis in fossil calcareous organisms. PhD Thesis, Columbia University, New York.

Wehmiller, J. F. 1980: Intergeneric differences in apparent racemization kinetics in mollusks and foraminifera: implications for models of diagenetic racemization. In Hare, P. E., Hoering, T. C. & King, K. Jr. (eds.): *Biogeochemistry of Amino Acids*, 305–356. J. Wiley, New York.

Wehmiller, J. F. 1982: A review of amino acid racemization studies in Quaternary mollusks: Stratigraphic and chronologic applications in coastal and interglacial sites, Pacific and Atlantic coasts, United States, United Kingdom, Baffin Island, and Tropical islands. *Quaternary Science Reviews 1*, 83–120.

Wehmiller, J. F. & Hare, P. E. 1971: Racemization of amino acids in marine sediments. *Science 173*, 907–911.

Williams, D. H. & Fleming, I. 1980: Spectroscopic methods in organic chemistry. 3rd ed. McGraw-Hill.

Williams, K. M. & Smith, G. G. 1977: A critical evaluation of the application of amino acid racemization to geochronology and geothermometry. *Origins of Life 8*, 91–144.

Wold, S. 1976: Pattern recognition by means of disjoint principal component models. *Pattern Recognition 8*, 127–139.

Wold, S. 1978: Cross validatory estimation of the number of components in factor and principal component models. *Technometrix 20*, 397–406.